

Dynamic Pulse Buckling of Imperfection-Sensitive Shells

Herbert E. Lindberg
APTEK, Inc., San Jose, California
December 8, 1989

Abstract

The theoretical basis of two related but distinctly different dynamic buckling criteria are summarized with the objective of demonstrating the range of applicability of each, so that together they cover the entire range of dynamic pulse loads from nearly impulsive loads to step loads of infinite duration. The example chosen is a cylindrical shell under elastic axial loads but the approach is applicable more generally. A critical amplification-of-imperfections criterion with a linear shell theory is shown to be applicable for short duration loads, for which a threshold nonlinear divergence criterion gives loads an order of magnitude too conservative. Conversely, the linear theory is inapplicable for long duration loads, for which critical loads are lower than the linear static buckling load because of imperfection sensitivity. In this range the threshold nonlinear divergence criterion is used. For loads of intermediate duration, an extended critical amplification criterion is used with equations that conservatively assume zero static buckling load but give an unchanged formula for critical load amplitude-duration combinations.

INTRODUCTION

A critical amplification criterion has been successfully applied to calculate dynamic pulse-buckling loads in a wide variety of structural elements (Lindberg and Florence, 1987), in each case with quite reasonable agreement with experimental loads for thresholds of dynamic buckling. In particular, critical loads for cylindrical shells under axial impact have been predicted for constant elastic axial stresses (Lindberg and Herbert, 1966), sustained constant axial plastic flow (Florence and Goodier, 1968), and oscillating elastic axial stresses (Lindberg, Rubin and Schwer, 1987). Buckling of cylindrical shells at elastic axial levels is very sensitive to initial imperfections. Under static loads, this sensitivity causes large changes in critical buckling stresses for almost imperceptible imperfections. In the present paper it is demonstrated that, under dynamic pulse loads, imperfection sensitivity does not strongly affect critical stress-duration combinations for buckling, but instead affects the range of stresses over which the theory can be applied.

Imperfection sensitivity under static axial loading has an extensive literature of research on the source of this sensitivity and methods of analysis. With the objective of avoiding duplication of this research for dynamic loads of long duration (step loads), Budiansky and Hutchinson (1964) developed a theory to relate critical dynamic loads to static buckling loads of imperfect shells, without specific reference to the imperfec-

tions themselves. They found expressions for the ratio of dynamic-to-static buckling loads as a function of the ratio of the static buckling load of the imperfect shell to the classical static buckling load of the perfect shell. They then extended this idea to pulse loads of finite duration (Hutchinson and Budiansky, 1966).

The buckling criterion used by Budiansky and Hutchinson is the transition from oscillatory motion under subcritical loads to divergent motion under buckling loads. For typical imperfect shells (static buckling loads about one fourth the classical loads), they found that critical step loads are about three fourths the slowly applied static load. For rectangular pulse loads of finite duration, their results were more complex, but toward the limit of short durations the critical condition reduces, of course, to a critical loading impulse. This is the same condition found by Lindberg and Herbert (1966), but the impulses from the critical amplification criterion are an order of magnitude larger than from the divergence criterion used by Budiansky and Hutchinson.

Roth and Klosner (1964) also found critical loads for cylindrical shells under axial rectangular pulse loads, based on a criterion of a sudden increase in nonlinear response amplitude, used by Budiansky and Roth (1960) for shallow spherical shells. Roth and Klosner's critical impulse for a cylindrical shell under short duration loads was only slightly larger than that given by Lindberg and Herbert, suggesting that, for short duration loads, their nonlinear response amplitude change criterion was similar to the critical amplification criterion.

In the present paper it is shown that the critical amplification criterion is the more appropriate for pulse loads, while the threshold divergence criterion is appropriate for step loads. An interpolation method is given for loads of intermediate duration. It is further suggested that, with the general source of imperfection sensitivity identified, the critical amplification criterion can be applied by knowing only the ratio of imperfect-to-perfect static buckling loads, just as for the threshold divergence criterion.

CRITICAL AMPLIFICATION THEORY

Equations of Motion

Both the threshold divergence and critical amplification criteria are applied to cylindrical shells by means of Donnell's equations, which in linear form are:

$$D\nabla^4 w + \bar{N}_x \frac{\partial^2}{\partial x^2} (w + w_i) + \rho h \frac{\partial^2 w}{\partial t^2} - \frac{1}{a} \frac{\partial^2 F}{\partial x^2} = 0 \quad (1)$$

$$\nabla^4 F = -\frac{Eh}{a} \frac{\partial^2 w}{\partial x^2} \quad (2)$$

where

$$\nabla^4 = \left(\frac{\partial^2}{\partial x^2} + \frac{\partial^2}{a^2 \partial \theta^2} \right)^2 \quad (3)$$

In these equations, x is axial coordinate, θ is circumferential coordinate, w is radial displacement, positive inward and measured from an unstressed initial displacement w_i , ρ is material density, E is Young's modulus, h is shell wall thickness, a is shell

radius, $D = Eh^3/12(1 - \nu^2)$ is shell bending stiffness, ν is Poisson's ratio, F is Airy's stress function for in-plane force resultants produced by the buckling deformation, and \bar{N}_x is the part of the axial force resultant from the applied axial load.

With dimensionless variables defined by

$$\xi = x \left(\frac{\bar{N}_x}{D} \right)^{1/2} \quad \eta = a\theta \left(\frac{\bar{N}_x}{D} \right)^{1/2} \quad \tau = \frac{\bar{N}_x}{(\rho h D)^{1/2}} \cdot t \quad (4)$$

Donnell's equations become

$$\nabla^4 w + \frac{\partial^2}{\partial \xi^2} (w + w_i) + \ddot{w} - \frac{1}{a \bar{N}_x} \frac{\partial^2 F}{\partial \xi^2} = 0 \quad (5)$$

$$\nabla^4 F = \frac{EhD}{a \bar{N}_x} \frac{\partial^2 w}{\partial \xi^2} \quad (6)$$

where now

$$\nabla^4 = \left(\frac{\partial^2}{\partial \xi^2} + \frac{\partial^2}{\partial \eta^2} \right)^2 \quad (7)$$

and dots indicate differentiation with respect to τ .

With simple-support boundary conditions

$$w = \partial^2 w / \partial x^2 = 0 \quad \text{at } x = 0, L \quad (8)$$

dynamic motion following sudden application of \bar{N}_x can be expressed by the Fourier series

$$w(\xi, \eta, \tau) = \sum_{m=1}^{\infty} \sum_{n=1}^{\infty} W_{mn}(\tau) \sin \alpha_m \xi \sin \beta_n \eta \quad (9)$$

$$F(\xi, \eta, \tau) = \sum_{m=1}^{\infty} \sum_{n=1}^{\infty} F_{mn}(\tau) \sin \alpha_m \xi \sin \beta_n \eta \quad (10)$$

in which

$$\alpha_m = \frac{m\pi}{L} \left(\frac{D}{\bar{N}_x} \right)^{1/2} \quad \beta_n = \frac{n}{a} \left(\frac{D}{\bar{N}_x} \right)^{1/2} \quad (11)$$

and the initial imperfections are also expanded into the Fourier series

$$w_i(\xi, \eta) = \sum_{m=1}^{\infty} \sum_{n=1}^{\infty} a_{mn} \sin \alpha_m \xi \sin \beta_n \eta \quad (12)$$

A similar set of equations results for imperfections of the form $b_{mn} \sin \alpha_m \cos \beta_n \eta$. With these expansions substituted into Donnell's equations 5–7, the equations of motion for the modal amplitudes W_{mn} are

$$\ddot{W}_{mn} + k(\alpha_m, \beta_n) W_{mn} = \alpha_m^2 a_{mn} \quad (13)$$

where

$$k(\alpha_m, \beta_n) = (\alpha_m^2 + \beta_n^2)^2 - \alpha_m^2 + \frac{1}{4} \left(\frac{\sigma_c}{\sigma} \right)^2 \frac{\alpha_m^4}{(\alpha_m^2 + \beta_n^2)^2} \quad (14)$$

The form for the multiplier in the last term of equation 14 follows from the observation that

$$\frac{EhD}{a^2 \bar{N}_x^2} = \frac{1}{4} \left(\frac{\sigma_c}{\sigma} \right)^2 \quad (15)$$

where σ is the axial stress from \bar{N}_x and

$$\sigma_c = \frac{Eh}{a} \frac{1}{\sqrt{3(1-\nu^2)}} \quad (16)$$

is the classical static buckling stress, which can be found by setting $k(\alpha_m, \beta_n) = 0$ and minimizing σ with respect to α_m and β_n treated as continuous variables.

Imperfection Growth and Buckling

The solutions to modal equations of motion 13 are

$$\frac{W_{mn}(\tau)}{a_{mn}} = \frac{\alpha_m^2}{k(\alpha_m, \beta_n)} \left[\begin{array}{c} \cosh p\tau \\ \cos p\tau \end{array} \right] \quad (17)$$

in which

$$p = |k(\alpha_m, \beta_n)|^{1/2} \quad (18)$$

The hyperbolic form is taken for $k(\alpha_m, \beta_n) < 0$ and the trigonometric form is taken for $k(\alpha_m, \beta_n) > 0$. For $k(\alpha_m, \beta_n) = 0$ the function multiplying α_m^2 is replaced by $\tau^2/2$, but this is seldom of concern because only in rare cases do α_m, β_n make k precisely zero with integer values m and n . The quantity given by the right side of equation 17 is called the ‘‘amplification function,’’ since it defines the amount by which the imperfection coefficients a_{mn} are amplified by dynamic motion.

If one were to use a threshold divergence criterion for this linear dynamic buckling motion, the dynamic buckling load would be simply the static buckling load, since it separates oscillatory motion from divergent motion. However, for finite duration pulse loads this criterion is far too conservative, as shown by the many examples of pulse buckling of structural elements in Lindberg and Florence (1987), and in particular for the cylindrical shell under axial loading (Lindberg and Herbert, 1966). With finite durations, loads with amplitudes far in excess of static buckling loads can be safely applied as long as the pulse duration is short enough that the magnitude of the motion remains acceptable. Experiments on a wide variety of structural elements have shown that motion is acceptably small if the amplification is less than about 25.

Lindberg and Herbert (1966) evaluated equation 17 over the range $\alpha_m, \beta_n < 2$ of significant amplifications, for τ ranging from 0 to 12. The most amplified mode is an axisymmetric mode with axial half-wavelength $\ell_x \approx \sqrt{2} \ell_0$, where $\ell_0 = \pi\sqrt{ah}/[12(1-\nu^2)]^{1/4}$ is the axisymmetric classical static buckle half-wavelength. This mode achieves an amplification of 25 at τ ranging only from 6 to 8 for σ/σ_c ranging from 1.1 to ∞ . Also, substantial growth occurs in hundreds of modes for thin shells. A statistical analysis showed that with uniformly distributed initial imperfections a_{mn} , the most probable wavelengths in the buckled form have an axial half-wavelength $\ell_x \approx \sqrt{2} \ell_0$ and a circumferential-to-axial wavelength ratio of $\ell_\theta/\ell_x \approx 3$ at these buckling times.

Measurements of permanent buckled forms and high-speed motion pictures showed wavelengths in good agreement with these predictions, and that at $\tau = 7$ buckles were just perceptible. It was therefore suggested that $\tau = 7$ be taken as a conservative buckling criterion, based on an amplification of about 25, essentially independent of σ/σ_c but with $\sigma/\sigma_c > 1$. Later in the present paper it is suggested that the latter condition can be relaxed to $\sigma/\sigma_{ds} > 1$, where σ_{ds} is the dynamic buckling load of the imperfect shell under step loading, from the threshold divergence criterion, for which $\sigma_{ds}/\sigma_s < 1$ and σ_s is the static buckling stress of the imperfect shell.

From the definition of τ in equation 4, the critical condition $\tau = 7$ at $t = T$ gives

$$\bar{N}_D T = 7(\rho h D)^{1/2} \quad (19)$$

or

$$\sigma_d T = \frac{7}{\sqrt{12}} \rho c h \approx 2\rho c h \quad (20)$$

where $c = \sqrt{E/\rho(1-\nu^2)}$ is the membrane wave speed in the shell, \bar{N}_D is the critical dynamic resultant force at duration T , and σ_d is the corresponding dynamic stress. Thus, threshold buckling deformations occur at a critical impulse imparted by the axial load. Also, because of the insensitivity to σ/σ_c noted previously, $\sigma_d T$ does not depend on a .

NONLINEAR DIVERGENCE THEORY

Equations of Motion

The initial work of Budiansky and Hutchinson (1964) focused on buckling from step loads, which is essentially a dynamic perturbation of static buckling since the load is maintained indefinitely. Thus, they used Koiter's (1963) theory of elastic stability and postbuckling behavior to capture the transition from small deformations at subcritical loads to large deformations when a critical buckling load is exceeded, just as for static buckling of imperfection sensitive shells. With a nonlinear form of Donnell's equations, they focused on analysis of motion in two modes, with ζ_1 taken as the amplitude of motion in the axisymmetric classical buckling mode and ζ_2 taken as the amplitude of a nonaxisymmetric classical buckling mode with equal axial and circumferential wavelengths [half wavelengths $\ell_x = \ell_\theta = 2\ell_0$; see for example Lindberg and Florence (1987) pp. 284-285]. Experiments reported by Almroth, Holmes and Brush (1964) demonstrate that initial buckling indeed occurs in this mode for step loading, produced in these experiments by a small lateral perturbation impulse applied to a statically loaded shell. (A suddenly introduced additional "imperfection" is not the same as a suddenly applied load, but the resulting dominant response modes are the same.)

With ζ_1 and ζ_2 expressed as fractions of the wall thickness, the equations of motion were found to be

$$\frac{1}{4} \ddot{\zeta}_1 + \left(1 - \frac{\lambda}{\lambda_C}\right) \zeta_1 - \frac{3b}{32} \zeta_2^2 = \frac{\lambda}{\lambda_C} \bar{\zeta}_1 \quad (21)$$

$$\ddot{\zeta}_2 + \left(1 - \frac{\lambda}{\lambda_C}\right) \zeta_2 - \frac{3b}{2} \zeta_1 \zeta_2 = \frac{\lambda}{\lambda_C} \bar{\zeta}_2 \quad (22)$$

where λ is the applied axial stress, λ_C is the classical static buckling stress given by equation 16, $b = [3(1 - \nu^2)]^{1/2}$, and $\bar{\zeta}_1$ and $\bar{\zeta}_2$ are imperfections, also as fractions of the wall thickness. (The notation ζ and b is used here rather than ξ and c as in the Budiansky and Hutchinson papers, because of other use of these symbols in the present paper.) Finally, here dots now indicate differentiation with respect to $\tau = \omega_2 t$, where the vibration frequencies associated with the two modes in the unloaded shell are

$$\omega_1 = \sqrt{2} c/a \quad \text{and} \quad \omega_2 = c/a\sqrt{2} \quad (23)$$

which can be found from equation 13 with $\sigma = 0$ and wave numbers α_m and β_n corresponding to the half wavelengths given above for these modes.

Numerical analysis showed that minimum dynamic buckling loads based on a threshold divergence criterion (discussed more explicitly in the next subsection) occurred with $\bar{\zeta}_1 = 0$, but nevertheless with $\zeta_1 \neq 0$ because of the nonlinear coupling. Solutions to a good approximation for this case were obtained by neglecting the inertia term $\ddot{\zeta}_1/4$ in equation 21, which allows ζ_1 to be expressed in terms of ζ_2^2 from equation 21 and substituted into equation 22 to obtain the single nonlinear equation

$$\ddot{z}_2 + (1 - \lambda/\lambda_C) z_2 - \left[\frac{9b^2 \bar{\zeta}_2^2}{64(1 - \lambda/\lambda_C)} \right] z_2^3 = \lambda/\lambda_C \quad (24)$$

where $z_2 = \zeta_2/\bar{\zeta}_2$.

Hinged-Rod Model

Budiansky and Hutchinson further observed that the form of equation 24 is very similar to that of the two rigid rod, three-hinge column model of von Kármán, Dunn and Tsien (1940), with a mass and lateral cubic-softening spring attached to the central hinge. The mass is M , the length of each rod is L_r , and the nonlinear spring force from lateral displacement u is

$$F = KL_r(\zeta - B\zeta^3), \quad B > 0 \quad (25)$$

With notation analogous to that for the shell, namely $\zeta = u/L_r$, and P and $P_C = KL_r$ denoting axial force and zero-imperfection buckling load, respectively, the equation of motion is

$$\ddot{z} + (1 - P/P_C)z - B\bar{\zeta}^2 z^3 = P/P_C \quad (26)$$

where $z = \zeta/\bar{\zeta}$ and dots now indicate differentiation with respect to $t\sqrt{K/M}$.

For the imperfect structure, with $\bar{\zeta} \neq 0$, the equilibrium displacement increases with increasing load to a maximum and then decreases with further increases in load. States beyond the maximum are therefore unstable, and the maximum is the buckling load P_S of the imperfect structure. This load is found by omitting the \ddot{z} term in equation 26 and setting $dP/dz = 0$, which yields

$$(1 - P_S/P_C)^{3/2} = \frac{3\sqrt{3}}{2} B^{1/2} \bar{\zeta}(P_S/P_C) \quad (27)$$

The dynamic buckling load for step loading with $z = \dot{z} = 0$ at $t = 0$ is found by first using the identity $\ddot{z} = \dot{z} d\dot{z}/dz$ so that equation 26 can be integrated once to obtain

$$\dot{z}^2 + (1 - P/P_C)z^2 - \frac{1}{2} B\bar{\zeta}^2 z^4 = 2(P/P_C)z \quad (28)$$

At loads below the dynamic buckling load, the steady-state motion is periodic and equation 28 defines its limit cycle in phase space z, \dot{z} . The maximum value, z_{\max} , of this limit cycle occurs when $\dot{z} = 0$, which gives

$$(1 - P/P_C)z_{\max}^2 - \frac{1}{2} B\bar{\zeta}^2 z_{\max}^4 = 2(P/P_C)z_{\max} \quad (29)$$

The dynamic buckling load P_D is defined as the load for which the amplitude (and period) of this limit cycle is infinite, so the motion diverges rather than approaching a limit cycle. This occurs under the condition $dP/dz_{\max} = 0$ applied to equation 29, with the result

$$(1 - P_D/P_C)^{3/2} = \frac{3\sqrt{6}}{2} B^{1/2}\bar{\zeta}(P_D/P_C) \quad (30)$$

A key feature of this simple model is that the imperfection parameter $B^{1/2}\bar{\zeta}^2$ can be eliminated between equations 27 and 30, giving a relationship between the static and dynamic buckling loads with no explicit dependence on the imperfections. The result is

$$P_D/P_S = \frac{\sqrt{2}}{2} \left(\frac{1 - P_D/P_C}{1 - P_S/P_C} \right)^{3/2} \quad (31)$$

By a similar procedure, the static buckling load from equation 24 for the cylindrical shell is given by

$$(1 - \lambda_S/\lambda_C)^2 = \left[\frac{9\sqrt{3}b}{16} |\bar{\zeta}_2| \right] (\lambda_S/\lambda_C) \quad (32)$$

and the dynamic buckling load is given by

$$\lambda_D/\lambda_S = \frac{\sqrt{2}}{2} \left(\frac{1 - \lambda_D/\lambda_C}{1 - \lambda_S/\lambda_C} \right)^2 \quad (33)$$

Plots in Budiansky and Hutchinson (1964) of P_D/P_S vs. P_S/P_C from equation 31 and λ_D/λ_S vs. λ_S/λ_C from equation 33 are very similar, the only difference being slightly more curvature in the plot from equation 33 than from equation 31 because of the larger exponent. Similar results were also found for the rigid-rod model with a quadratic- rather than cubic-softening spring, which gives the same exponent as in equation 33 but a coefficient $3/4 = 0.75$ in place of $\sqrt{2}/2 = 0.707$.

Critical Finite Duration Loads

In Hutchinson and Budiansky (1966), the equations of motion of the rigid-rod model for both the quadratic- and cubic-softening springs were integrated numerically for rectangular and triangular (sudden jump in load followed by linear decay to zero) finite-duration pulse loads. For each model and pulse shape, they again gave plots of

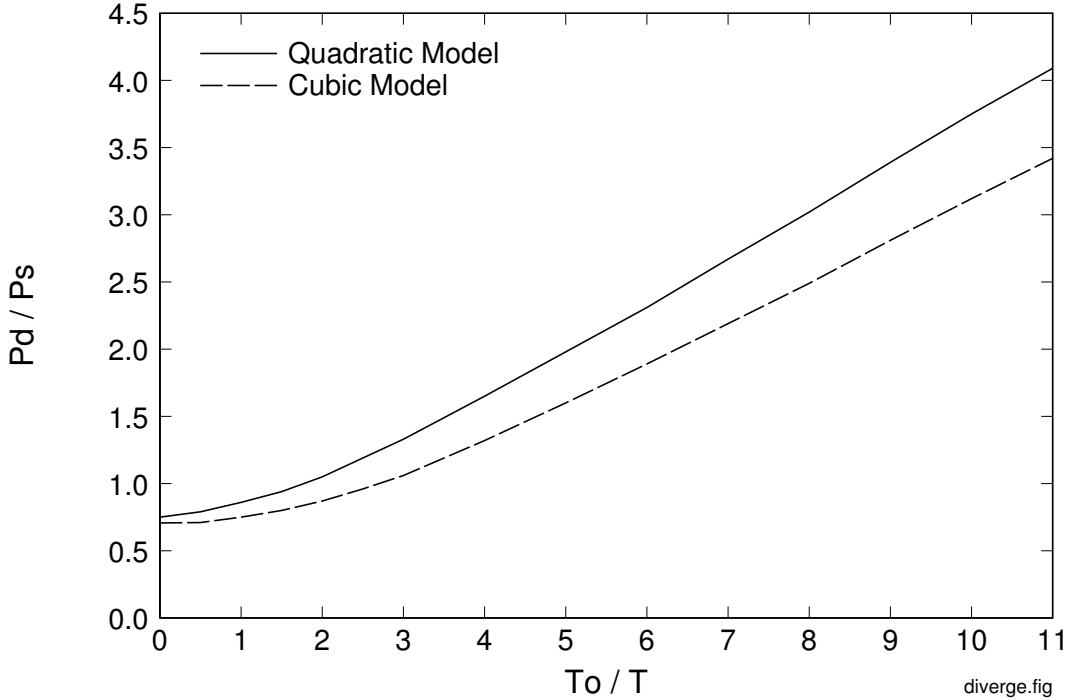


Figure 1: Conservative dynamic buckling estimates ($\lambda_S/\lambda_C = 0$) from the threshold divergence theory, rectangular loading.

λ_D/λ_S vs. λ_S/λ_C but with pulse duration as a parameter, found by use of a divergence threshold criterion just as for step loads. These curves showed a rapid increase in finite duration critical loads with λ_S/λ_C increasing beyond about 0.2, suggesting a high sensitivity of critical dynamic loads to imperfections. In the present paper it is shown that, with the more appropriate critical amplification criterion, critical short pulse loads are insensitive to imperfections for any value of λ_S/λ_C .

For conservative practical application, curves were given of λ_D/λ_S vs. T_0/T for the limiting case of imperfect shells with $\lambda_S/\lambda_C \rightarrow 0$, based on the observation that for $\lambda_S/\lambda_C < 0.2$ critical dynamic load ratios λ_D/λ_S are weakly dependent on λ_S/λ_C . The time T_0 is the vibration period of the dynamic buckling mode in the absence of loading, and T is the rectangular pulse duration. These are repeated here in Figure 1. The curves approach the static results of Budiansky and Hutchinson (1964) as $T_0/T \rightarrow 0$, and approach straight lines toward the impulsive loading limit $T_0/T \rightarrow \infty$.

For the cubic model, which more closely approximates the behavior of the cylindrical shell equation (24), a straight line approximation $\lambda_D/\lambda_S = T_0/T$ can be used to good accuracy for $T_0/T > 3$. With $T_0 = 2\pi/\omega_2$, and $\omega_2 = c/a\sqrt{2}$ from equation 23 and $\sigma_c = Eh/a\sqrt{3(1-\nu^2)}$ from equation 16, this line gives the following simple formula for critical dynamic axial buckling stress

$$\sigma_d = \pi \left(\frac{2}{3}\right)^{3/2} \frac{\rho ch}{T} \cdot \frac{\sigma_s}{\sigma_c} \quad (34)$$

or

$$\sigma_d T = 1.71 \rho ch (\sigma_s/\sigma_c) \quad (35)$$

For a typical static buckling load ratio $\sigma_s/\sigma_c \approx 0.25$, equation 35 gives $\sigma_d T = 0.43 \rho ch$. If one uses the symmetric mode period from ω_1 in equation 23 as the more conservative estimate suggested by Hutchinson and Budiansky (1966), then the coefficient in equation 35 becomes $1.71/2 = 0.855$. With this more conservative buckling mode period, $\sigma_d T = 0.21 \rho ch$. These are in exactly the same form as given by equation 20 from the amplification criterion but with a coefficient an order of magnitude smaller. If one were to use for T_0 the period from the most amplified mode, a symmetric mode with half wavelength $\ell_x = \ell_0/\sqrt{2}$, the coefficient would be even smaller.

CHOICES OF BUCKLING CRITERIA

The excellent agreement between experimental results and critical loads based on a critical amplification criterion suggests that for relatively short finite duration loads this criterion is more appropriate than the threshold divergence criterion. Furthermore, the formula $\sigma_d = 2 \rho ch$ is also the formula for a bar or flat plate, which corresponds to $a \rightarrow \infty$. Thus, there is no reason to suspect that the critical amplification formula is unconservative because of any peculiarity of complex nonlinear shell response; the finite radius of the shell makes the shell “stiffer” than the plate. In the physical buckling process, a sudden-jump dynamic load is applied by impact, and divergent flexural motion takes place only while the stress pulse is maintained. If the shell has a free boundary condition at the opposite end, as in Lindberg and Herbert (1966), then following the compressive pulse the stress jumps to a tensile stress equal to the initial compression and not to zero as assumed in Hutchinson and Budiansky (1966).

Furthermore, as time proceeds, axial waves continue to reverberate between one end of the shell and the other. For the case with one end impacted and fixed to a heavy mass and the other end free, these reverberations result in alternating compressive and tensile pulses near the impacted end of the shell, where the flexural motion is largest. Lindberg, Rubin and Schwer (1987) showed that further buckling occurs during the first two or three compressive pulses, interspersed by oscillatory motion during the tensile pulses. Also, the corresponding change of the equations of motion between hyperbolic and elliptic forms results in buckle growth fixed in space during the compressive pulses and bending wave propagation away from the impacted end during the tensile pulses. This spread in bending energy during the tensile pulses, together with the finite membrane energy available in the initial compression wave, limits the amount of buckle growth from later compressive pulses such that the single-pulse formula in equation 20 still gives a reasonable estimate for critical impact loading, with T taken as the single round trip transit time of an axial stress wave.

If the shell has an axially fixed boundary at the end opposite the impact, then the compressive stress increases with each axial stress wave reverberation between the impacted and fixed end, resulting eventually in long duration dynamic loading. This is closer to the situation analyzed in Budiansky and Hutchinson (1964), but no attempt was made there to define how one would obtain a sudden increase in load to a fixed load of constant magnitude. The implicit assumption is that the analyst is seeking a conservative estimate for a dynamically applied load and that a step load

is a conservative idealization of actual loading through a short series of axial wave reverberations. Thus, in these cases the threshold divergence criterion is appropriate.

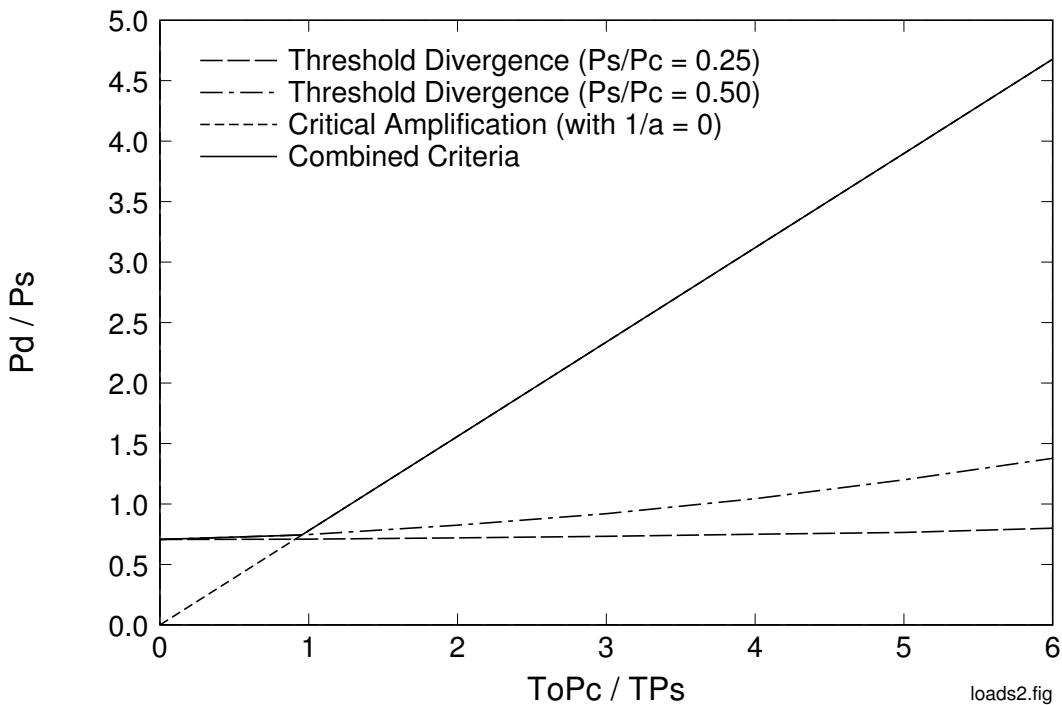


Figure 2: Dynamic buckling loads for cylindrical shells under rectangular pulse loads of duration T (Here, T_0 is the unloaded vibration period of the classical axisymmetric buckling mode.)

CRITERIA FOR INTERMEDIATE PULSE DURATIONS

In place of Figure 1, the combined criteria scheme given in Figure 2 is suggested. The short-dashed line (and the solid extension superimposed on it) is from the critical amplification criterion, given in the form

$$\frac{P_D}{P_S} = \frac{\sqrt{6}}{\pi} \left(\frac{T_0}{T} \right) \left(\frac{P_C}{P_S} \right) \quad (36)$$

which is equation 20 with T_0 taken as the free vibration period $\sqrt{2}\pi a/c$ of the axisymmetric classical buckling mode. (The extension of applicability to $P_D/P_C < 1$ is made with the conservative assumption that for pulse buckling one can consider that $1/a = 0$, so that an effective $P_C^{\text{eff}} \rightarrow 0$, as discussed more fully in the following paragraphs.) The long-dashed and dash-dot curves are from the threshold divergence criterion for imperfections such that $P_S/P_C = 0.25$ and 0.50 , respectively. These are essentially the cubic model curve from Figure 1 with the T_0/T abscissa stretched out to the new abscissa definition in Figure 2, but with a slight increase in P_D/P_S because of the effect of P_S/P_C as given in Hutchinson and Budiansky (1966).

The combined criteria curve is the solid curve, taken as the upper envelope of the two criteria because each criterion is conservative. This solid curve consists essentially of the critical amplification curve for P_D greater than the step buckling load $P_D/P_S = \sqrt{2}/2$ given by equation 31 (or equation 33) for $P_S/P_C \rightarrow 0$. For longer pulse durations (smaller T_0/T), this straight line is terminated and the critical load is taken as the conservative value $P_D/P_S = \sqrt{2}/2$ from the step-load theory. For common shells in which $P_S/P_C \approx 0.25$, the corner of the resulting plot occurs at a pulse duration $T \approx 4T_0$. For a one meter diameter shell, $T \approx 4\sqrt{2}\pi(1\text{ m})/5000\text{ m/s} = 0.00355\text{ s}$.

For values of T_0P_C/TP_S “near” but greater than the intersection point 0.907, the dynamic-to-static classical buckling load ratio $P_D/P_C = (P_D/P_S)(P_S/P_C)$ is less than 1 but lies on the critical amplification portion of the plot in Figure 2. For example, with $P_S/P_C = 0.25$, $P_D/P_C < 1$ for $T_0P_C/TP_S < 5.2$. In this range, the roots $k(\alpha_m, \beta_n)$ from equation 14 are positive and response is oscillatory rather than divergent. In this range we appeal to the nonlinear equations of motion 21 and 22 which, by definition of P_S/P_C in equation 32, give unstable motion for all points on the plot in Figure 2. However, we continue to use $\sigma_d T$ calculated on the basis of a critical amplification rather than threshold divergence, which has been shown to be too conservative. One method to visualize this approach is to conservatively take $\sigma_c/\sigma = 0$ in equation 14, which as mentioned previously leads to the same critical impulse formula $\sigma_d T = 2\rho ch$ as for finite σ_c .

Beyond this appeal to the nonlinear equations of motion, there are two other physical processes that result in divergent motion for $\sigma/\sigma_c < 1$. The first is the quasi-nonlinearity of an increase in the local radius of curvature a because of imperfections in modes with wavelengths longer than for the dynamic modes of response. From equation 16, this increase results in a local decrease in σ_c over portions of the shell where imperfections so combine. Calculations of curvature changes with imperfection amplitudes given in Arbocz (1982) give static buckling load reductions of 10 to 20% just from this effect. The basis of these calculations and comparisons of buckling load reductions from nonlinear effects (equation 32) and from curvature changes are given in the Appendix.

The second additional source of divergent motion for $\sigma/\sigma_c < 1$ is from hoop stresses produced by the Poisson effect for dynamic loading. Even small hoop stresses result in divergent motion. For the shell with $a/h = 500$, $L/2a = 1.62$ in Lindberg, Rubin and Schwer (1987), calculations there showed that the Poisson effect reduced the critical load separating oscillatory from divergent motion to $\sigma_{cr}/\sigma_c = 0.204$, for the $m = 1, n = 4$ mode. However, these hoop stresses are quickly relieved because the shell is free to expand. The duration of the initial hoop stress pulse for impact loading is the quarter period $\pi a/2c$ of the breathing mode. The value of τ with $\bar{N}_\theta = \nu \bar{N}_x$ for this period and $\nu = 0.3$ is $0.98 \sigma/\sigma_c$, so initial growth from the Poisson effect is small. Nevertheless, for the multi-pulse loading in Lindberg, Rubin and Schwer (1987), the duration of the next compressive swing of the hoop mode is the half period. Strain measurements for an impact load $\sigma/\sigma_c = 0.87$ showed both axial and circumferential flexural growth during the second circumferential compressive pulse.

SUMMARY AND CONCLUSIONS

A linear critical amplification criterion applied to dynamic buckling from pulse loads gives conservative estimates for combinations of stress amplitude and duration that can be safely applied with only modest flexural motion. A nonlinear threshold divergence criterion applied to these same pulse loads gives amplitude-duration combinations an order of magnitude less than from the critical amplification criterion. The latter criterion is therefore overly conservative for these relatively short pulse loads. Conversely, for long duration loads the linear critical amplification criterion is unconservative because *linear* divergence and hence buckle growth occurs only for $\sigma/\sigma_c > 1$. For long duration loads the nonlinear threshold divergence criterion is appropriate. For loads of intermediate duration the linear critical amplification criterion is made conservative (but not as conservative as the nonlinear threshold divergence criterion) by letting $\sigma_c = 0$ in the equations of motion, which allows the formula from this criterion to be applied to all loads with $\sigma/\sigma_{ds} > 1$, where σ_{ds} is the dynamic buckling load from the nonlinear threshold divergence criterion for step loads. The two criteria then give dynamic buckling loads that are not overly conservative over the entire range of pulse durations for which critical stresses are elastic. Furthermore, no specific reference is made to imperfections in either dynamic theory, so imperfection sensitivity need be investigated in detail only for static buckling.

REFERENCES

- Almroth, B. O., Holmes, A. M. C., and Brush, D. O., 1964, "An Experimental Study of the Buckling of Cylinders Under Axial Compression," *Exptl. Mech.*, **4**, pp. 263-270.
- Arbocz, J., 1982, "The Imperfection Data Bank, A Means to Obtain Realistic Buckling Loads," *Buckling of Shells, Procedures of a State-of-the-Art Colloquium*, Springer-Verlag, New York.
- Budiansky, B., and Hutchinson, J. W., 1964, "Dynamic Buckling of Imperfection-Sensitive Structures," *Proc. 11th Int. Congress of Appl. Mech.*, Springer-Verlag, Berlin, pp. 636-651.
- Budiansky, B., and Roth, R. S., 1960, *Axisymmetric Dynamic Buckling of Clamped Shallow Spherical Shells*, NASA Technical Note D-1510 (1960).
- Florence, A. L., and Goodier, J. N., 1968, "Dynamic Plastic Buckling of Cylindrical Shells in Sustained Axial Compressive Flow," *ASME Trans., Series E, J. Appl. Mech.*, **35**, pp. 80-86.
- Hutchinson, J. W., and Budiansky, B., 1966, "Dynamic Buckling Estimates," *AIAA Journal*, **4**, 3, pp. 525-530.
- von Kármán, T., Dunn, L. G., and Tsien, H. S., 1940, "The Influence of Curvature on the Buckling Characteristics of Structures," *J. Aerospace Sci.*, **7**, pp. 276-289.
- Koiter, W. T., 1963, "Elastic Stability and Post-Buckling Behavior," *Non Linear Problems*, ed. R. E. Langer, U. Wisconsin Press, Madison, WS.
- Lindberg, H. E., and Herbert, R. E., 1966, "Dynamic Buckling of a Thin Cylindrical Shell Under Axial Impact," *ASME Trans., Series E, J. Appl. Mech.*, **33**, pp. 105-112.

Lindberg, H. E., and Florence, A. L., 1987, *Dynamic Pulse Buckling—Theory and Experiment*, Martinus Nijhoff, Dordrecht, The Netherlands.

Lindberg, H. E., Rubin, M. B., and Schwer, L. E., 1987, “Dynamic Buckling of Cylindrical Shells from Oscillating Waves Following Axial Impact,” 1987, *Int. J. Solids Structures*, **23**, 6, pp. 669-692.

Roth, R. S., and Klosner, J., 1964, “Nonlinear Response of Cylindrical Shells Subjected to Dynamic Axial Loads,” *AIAA Journal*, **2**, 10.

APPENDIX

Static buckling loads are reduced by the combined effects of imperfections and nonlinearities, such as given by equation 32, and also by a direct change in the local curvature of the shell caused by imperfections. Since the latter allows straightforward use of the critical amplification criterion for $\sigma < \sigma_c$, it is useful to explore the magnitude of both mechanisms of static buckling load reduction.

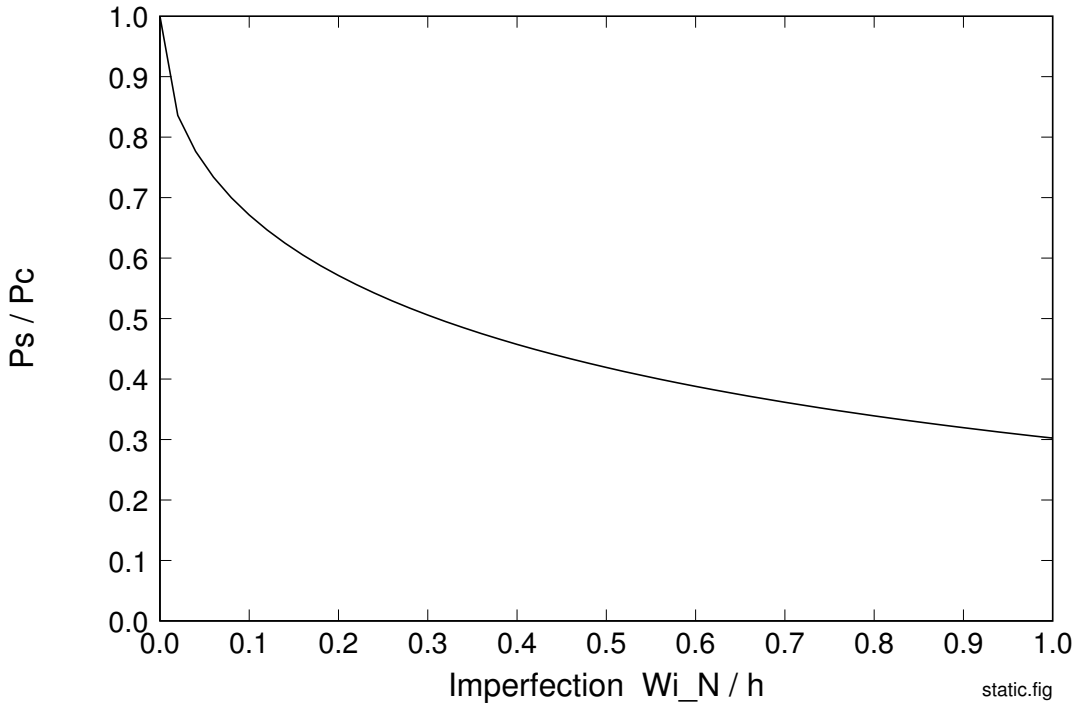


Figure 3: Static buckling load reduction caused by nonlinear mode-coupling with imperfections in the square classical buckle mode.

Figure 3 gives the static buckling load reduction from imperfections in the square classical buckle mode, calculated from equation 32. The buckling load decreases abruptly for imperfections only a few percent of the wall thickness, and then decreases more slowly for larger imperfections. A reduction to 30% of the classical buckling load would require an imperfection equal to the wall thickness for this limited theory.

Reductions from curvature change are not as precipitous as for nonlinear response, but the reductions continue steadily with large imperfections rather than tapering off as for nonlinear response, so if imperfections are a substantial fraction of the wall thickness (crudely made shells, or shells damaged in service) the curvature change could become the dominant effect of imperfections.

The local curvature of the imperfect shell is given by

$$\frac{1}{a_s(x, \theta)} = \frac{1}{a} + \frac{w_i}{a^2} + \frac{\partial^2 w_i}{a^2 \partial \theta^2} \quad (\text{A-1})$$

For this purpose, it is convenient to express the initial imperfections in the form

$$w_i(x, \theta) = a \sum_{m=1}^{\infty} \sum_{n=1}^{\infty} \gamma_{mn} \sin \frac{m\pi x}{L} \sin(n\theta + \phi_n) \quad (\text{A-2})$$

where $\gamma_{mn} = (a_{mn}^2 + b_{mn}^2)^{1/2}/a$ and ϕ_n is the phase angle of the n^{th} mode imperfection. With the w_i/a^2 term neglected as small, equation A-1 with equation A-2 gives

$$\frac{1}{a_s} = \frac{1}{a} - \frac{1}{a} \sum_{m=1}^{\infty} \sum_{n=1}^{\infty} n^2 \gamma_{mn} \sin \frac{m\pi x}{L} \sin(n\theta + \phi_n) \quad (\text{A-3})$$

Consider a specific location some distance from the end of the shell to avoid the complexity of summing over m , and then replace γ_{mn} by $\bar{\gamma}_n$. Also, from equation 16, the local static buckling load is $\sigma_s/\sigma_c = a/a_s$, so

$$\frac{\sigma_s}{\sigma_c} = 1 - \sum_{n=1}^{N/2} n^2 \bar{\gamma}_n \cos(n\theta + \phi_n) \quad (\text{A-4})$$

With static buckling in the square classical mode having $n = N$, imperfection modes up to only half this number are included in the final sum expression, to ensure that the local curvature encompasses a buckle. The half wavelength at $n = N$ is $2\ell_0$, so

$$\frac{\pi a}{N} = 2\pi \sqrt{ah} [12(1 - \nu^2)]^{1/4} \quad (\text{A-5})$$

or, with $\nu = 0.3$,

$$N = 0.91 \sqrt{a/h} \quad (\text{A-6})$$

If one assumes that the imperfections are introduced by random processes, the phase angles ϕ_n can be taken as random and uniformly distributed. The mean value of the curvature change is therefore the root-mean-square of the coefficients in equation A-4. Somewhere on the shell the curvature change will be as large as about three times this value, so

$$\left. \frac{\sigma_s}{\sigma_c} \right|_{\min} \approx 1 - 3 \left[\sum_{n=1}^{N/2} (n^2 \bar{\gamma}_n)^2 \right]^{1/2} \quad (\text{A-7})$$

Data from Arbocz (1982) suggests that values for $\bar{\gamma}_n$ can be approximated by $\bar{\gamma}_n = A/n$, where A is about 0.0015. The formula applies only for $n > 8$, below which

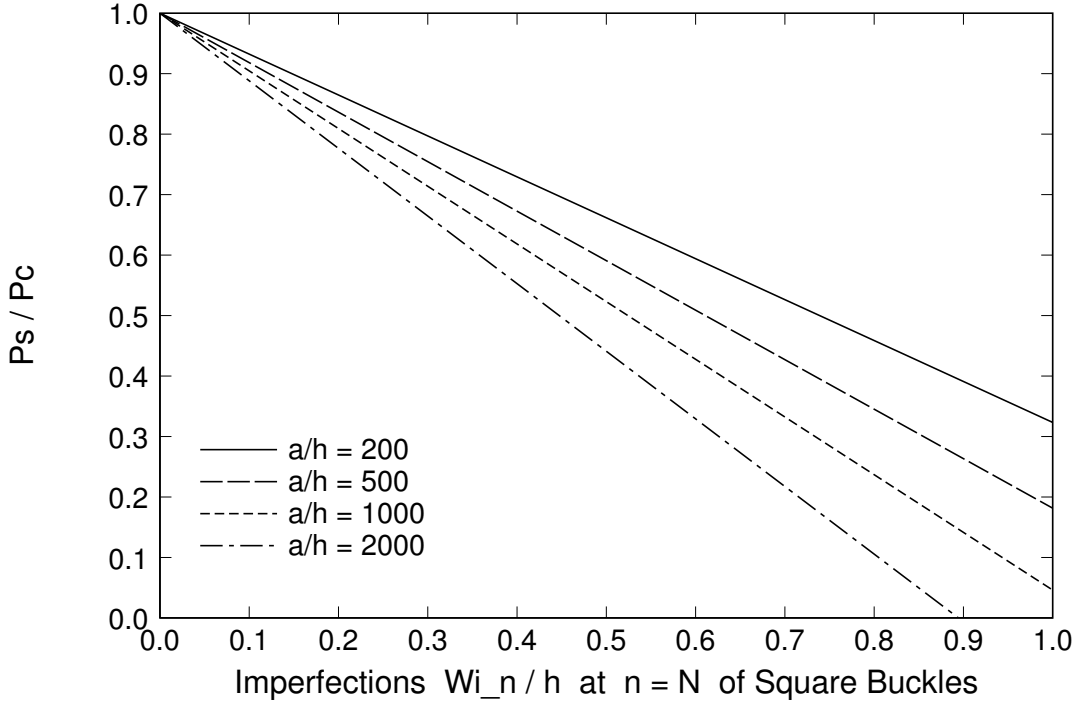


Figure 4: Static buckling load reduction caused by local curvature reductions from modal imperfections varying as $1/n$.

imperfections are nearly constant, but since $\bar{\gamma}_n$ is multiplied by n^2 in equation A-7 and $N/2 \gg 8$ for the thin shells discussed here, this cutoff is neglected for simplicity. Then, with $\bar{\gamma}_n = A/n$, equation A-7 becomes

$$\left. \frac{\sigma_s}{\sigma_c} \right|_{\min} \approx 1 - 3A \left[\frac{M(M+1)(2M+1)}{6} \right]^{1/2} \quad (\text{A-8})$$

in which the expression under the root is the sum of n^2 to $M = N/2$. For $a/h = 1000$, $N = 30$ and $\sigma_s/\sigma_c = 0.84$ for $A = 0.0015$. Thus, for shells of the type described in Arbocz (1982), reductions in buckling loads of about 10 to 20% are expected from local curvature changes. From equations A-6 and A-7, this reduction varies as $(a/h)^{1/2}$.

If imperfections are as large as required for substantial buckling load reduction in Figure 3 from nonlinear effects, reductions from curvature changes are also substantial. This is shown in Figure 4, which was constructed by again taking a $1/n$ variation of imperfection amplitudes and summing to $N/2$, but with $A = N\bar{\gamma}_N$, where $\bar{\gamma}_N = \bar{\zeta}_2 h/a$ and $\bar{\zeta}_2$ is the value of the abscissa w_{iN}/h in Figure 3. In evaluating equation A-8 for this plot, the 3-sigma factor was omitted, to be reasonably consistent with the effective value of $\bar{\zeta}_2$ in Figure 3 being the highest local value for $n = N$, so $\bar{\zeta}_2$ already contains such a factor. Although this necessarily is a crude comparison because of the vagaries of imperfections, it is reasonable to conclude that for large imperfections curvature change effects must be considered in addition to nonlinear effects.